Contents list available at CBIORE journal website

International Journal of Renewable Energy Development

Journal homepage: https://ijred.cbiore.id

Research Article

An innovative air-cooling system for efficiency improvement of retrofitted rooftop photovoltaic module using cross-flow fan

Rozita Mustafa[a,b,c], Mohd Amran Mohd Radzi[a,b*], Hashim Hizam[a,b], Azura Che Soh[a]

[a]Department of Electrical and Electronic Engineering, Faculty of Engineering, Universiti Putra Malaysia, 43400 UPM Serdang, Selangor Darul Ehsan, Malaysia.

[b]Advanced Lightning, Power and Energy Research (ALPER) Centre, Universiti Putra Malaysia, 43400 UPM Serdang, Selangor Darul Ehsan, Malaysia.

[c]Electrical and Electronics Department, German Malaysian Institute, Jalan Ilmiah, Taman Universiti, 43000 Kajang, Selangor Darul Ehsan, Malaysia.

Abstract. . This study presents an innovative air-cooling photovoltaic (PV) system using cross-flow fan with speed regulation to optimize performance of rooftop PV system in tropical climates like Malaysia. Air passed through the impeller enters perpendicularly to the motor shaft, deflected by the fan blades and evacuated, allowing the fan to operate at its most efficient operating point. The airflow provided within the rear of the PV modules and the roof surface blow out the trapped hot air. Changes in the PV module temperature (T_{cell}) are detected and the fan speed are adjusted accordingly to the PWM. This method was tested for 12 hours continuously from 7:00 am on the existing PV system at German Malaysian Institute (GMI) Bangi. The highest T_{cell} achieved 72.88 °C and 55.75°C without and with air-cooling system with average power 210.22 W and 246.67 W per peak sun factor (PSF) respectively. There was a 17.34% increase in average power with a 13.18% in average net output power and achieved 6.68% energy efficiency using the proposed cooling system. T_{cell} increases more swiftly and reaches higher temperatures in the absence of a cooling system, whereas T_{cell} increases more slowly and at lower temperatures when a cooling system is present. The projected system's power rating was 6.48 W, which is 2.6% per PV module, and it really attained 6.32 W, which is 2.53% per PV module, while total energy consumption by the fan was 51.89 Wh per day, which is only 3.89% per PV module.

Keywords: uniform air-cooling, cross-flow fan, PV module temperature, cooling technique, photovoltaic

Check for updates

@ The author(s). Published by CBIORE. This is an open access article under the CC BY-SA license (http://creativecommons.org/licenses/by-sa/4.0/).

Received: 23rd Oct 2023; Revised: 17th January 2024; Accepted: 5th Feb 2024; Available online: 16th Feb 2024

1. Introduction

Due to the lack of risk and natural disasters, renewable energy is now seen as a more desirable source of fuel, with the world's energy consumption increasing at a rate of 3% per year (Rawat *et al.*, 2016). The favourable ecological impact of renewable energy sources makes them the preferred energy source for power generation (Adaramola, 2015). The PV technology that converts direct sunlight irradiance to electricity has gained tremendous appeal, particularly in places with high solar irradiance (Verma *et al.*, 2021). Moreover, the cost of *PV* systems has fallen below grid parity in many regions of the world (Vishal Shah, Jerimiah Booream-Phelps, 2014). Retrofitted mounting refers to the mounting of a *PV* system over the existing roof tiles, using brackets to elevate the solar panels above the roof (Yusoff *et al.*, 2017). A gap between *PV* modules and the roof restrict airflow through it. Building integrated *PV* (*BIPV*) mounting is when *PV* modules are integrated into a structure (Yusoff *et al.*, 2017). Besides reducing leakage, retrofit mounting is becoming an increasingly popular option (Union of Concerned Scientists, 2015). Rooftop *BIPV* installations are an excellent method of obtaining clean energy (Lee *et al.*, 2019) but they also have their own set of factors that can reduce their power output (Pandey *et al.*, 2022). There are some studies on the relationship between the immediately built environments such as roof type material and a gap between the *PV* modules and the roofs on the operating T_{cell}. *PV* modules become overheated due to the massive solar irradiance and high ambient temperature (Moharram *et al.,* 2013). Haidar et al. (Haidar et al., 2018) observed *PV* modules receiving solar energy as input and supplying electricity to the connected load with a significant amount of solar energy transformed into heat and lost through convection and radiation to the external environment. This heat at the *PV* module surface was released into the atmosphere and air gap on the backside of the PV module (Amelia *et al.*, 2016). Yusoff et al. (Yusoff *et al.*, 2017) found that the T_{cell} and the temperature difference (ΔT) are dependent on the roofing material type, *PV* technologies, irradiance and the gap height in between the *PV* module and roof surface. The amount of energy generated by these rooftop solar arrays depends on a variety of factors, including the weather, the design, and the arrangement and alignment of the PV modules (Pandey *et al.*, 2022). The performance of *PV* modules degrades significantly as their operating temperature rises (Haidar *et al.*, 2018). Open circuit voltage, V_{OC} decreases substantially as the ambient temperature of the solar PV cell rises above 25^0C. With a decrease in operating temperature, the *PV* module's electrical output increases and the overall amount of power generated increases. Fatoni et al. (Fatoni *et al.*, 2019)

* Corresponding author
Email: amranmr@upm.edu.my (M.A. M. Radzi)

https://doi.org/10.61435/ijred.2024.60068
ISSN: 2252-4940/© 2024.The Author(s). Published by CBIORE

have reported in their study that a 0.5% decrease in efficiency resulted for every 1^0C rise in operating T_{cell}. To sustain a suitable temperature, a cooling system is necessary to remove solar heat that produces PV heating (Hamzat *et al.*, 2021). An integrated PV cooling system during operation is a very important task for improving PV system performance (Elminshawy, El Ghandour, et al., 2019) and it has been demonstrated that significant power gains are possible, up to a total of 5 % (Smith *et al.,* 2014) by utilization of a cooling system. The higher electrical performance in PV systems can reduce the payback time of the invested capital (Hussien *et al.*, 2015; Jie Ji, Jian-Ping Lu, Tin-Tai Chow, Wei He, 2007).

2. Cooling techniques for PV module

As only 13% to 15% of solar irradiance is converted into electricity, cooling is required to increase the efficiency of PV modules and decrease energy loss in the form of heat (Mattei et al., 2006). To minimize the operating T_{cell}, it is necessary to eliminate heat energy. Consequently, the operating T_{cell} can be maintained close to the ambient temperature (T_{amb}), (Amelia *et al.,* 2016). Cooling of the PV module is important to eliminate excess heat effects and ensure that efficient output power can be achieved. Many methods for cooling PV modules have been proposed. These include natural air, forced air, water, phase change materials (PCM), thermoelectric cooling, transparent coating, and evaporative cooling (Haidar *et al.*, 2018).

Two types of cooling can be categorized that is active cooling, which consumes energy and the second is passive cooling, which uses natural convection/conduction to remove extra heat. The most common passive cooling approach for PV modules is the installation of aluminium fins and a heat sink on the module's backside surface. Hernandez *et al.* (Hernandez-Perez *et al.*, 2021), utilised a passive heatsink design for PV module cooling in numerical modelling and found a temperature reduction up to 7^0C. Grubišić Čabo et al. (Grubišić Čabo *et al.*, 2020) improved the maximum power output of the PV system by 5% after applying perforated aluminium fins to the back surface of the PV module. Elbreki *et al.* (Elbreki *et al.,* 2020) experimented by combining a planar reflector and backplate expanded surface on the PV module and increased the electrical efficiency to 11.2 %. Idoko *et al.* (Idoko *et al.*, 2018) recommended a cooling strategy that incorporated both surface water cooling and an aluminium heat sink at the back of the same module, resulting in a 3% gain in efficiency.

The phase change material (PCM) as cooling systems have gained popularity in recent years due to the reduction in T_{cell} and improvement in performance. Abdulmunem *et al.* (Abdulmunem *et al.*, 2021) considered heat transfer by using a PCM as a passive cooling technique and showed little cooling performance at a lower tilt angle. Sharma et al. (Sharma et al., 2021) studied convective PV modules and PV/T systems utilising PCM and determined that the electrical efficiency of $PV/T\ PCM$ would be 10.2 % higher. In an experiment by Sudhakar et al. (Sudhakar *et al.*, 2021), a combination of PCM and a natural water-cooling system was utilized and prove a yielding average temperature reduction of 11.92 %, a maximum overall exergy production of 12.4 % and an exergy efficiency of 13.54 %. Sethiya *et al.* (Sethiya, 2021) comes up with an idea of the jacket attached to the back of the PV module and stuffed with glycerol and results in a 0.4 % loss in the efficiency of PV modules.

Zubeer and Ali (Zubeer & Ali, 2021) added two reflectors side by side and used a 45 $W\ ac$ water pump to move water from a tank to a pipe attached to the top end of the front side of the PV module and enhanced 17.7% the electrical performance. Gomaa *et al.* (Gomaa *et al.*, 2020) used both active and passive cooling by spraying water in front of the PV module surface and mounting fins on the back. Daily energy harvesting increased by 10.2%. Dida *et al.* (Dida et al., 2021) conducted research on passive cooling through water evaporation and the capillary action of a burlap cloth attached directly to the module's rear surface. This technique was successful, resulting in a substantial 14.75% increase in electrical efficiency. Castanheira *et al.* (Castanheira *et al.*, 2018) prototype's active cooling technique was tested by installing it on a 5 kW (25-panel) PV solar power plant string. Low-pressure water is sprinkled along the PV panels to ensure uniform distribution and reduce water leakage. The proposed technique increased annual energy production by as much as 2 % and increased maximum power by 17 %. Joseph *et al.* (Joseph Paul *et al.*, 2021) sprinkled low pressure water along the PV module and introduced a double-sided cooling system that improved performance and efficiency by 7.7%.

When water is used as a cooling method on an existing PV system, it is imperative to carefully determine the optimal placement of the water source on the rooftop. If the water source is located close to the existing PV system, the water storage will be exposed to solar irradiance, which will cause the water temperature to rise and render it unsuitable for cooling. For this, a method should be devised to deliver water from the source to the PV system area involving water pressure, material used to prevent the water from absorbing excessive heat, and energy required for this process. The used water permitted to flow onto the roof and the long-term impact of exposing the roof to excessive humidity and moisture should be considered. The possibility of roof leaks or the created gutter channel for spent water will therefore lead to modifications to the current PV system and the associated expenditures.

Although air is less efficient than liquid as a coolant, it has some advantages such as low material consumption and operating costs (Tonui & Tripanagnostopoulos, 2007). Kaewchoothong *et al.* (Kaewchoothong *et al.*, 2021) designed multiple cooling modules with rib turbulators installed at the rear of the PV module to uniformly cool and improve the PV module's performance. Their active air-cooling design increased average output power by more than 13.97%. Lebbi *et al.* (Lebbi *et al.*, 2021) improved electrical efficiency by forcing air circulation on the backside of the PV module and flowing water on the front surface. Lebbi incorporated active cooling with self-cleaning and the use of Bi-Fluid coolants into the design and proposed current hybrid system to improve solar pumping irrigation as future work. Kabeel *et al.* (Kabeel *et al.*, 2019) applied technologies for both forced-air and water-cooling in the presence of reflectors research. The result demonstrated a gain in net output electricity. Elminshawy et al. (Elminshawy, Mohamed, *et al.,* 2019) utilised an earth-to-air heat exchanger ($EAHE$) to precool the ambient air, which was then used to cool the back surface of the PV panel. The result demonstrated an average increase in PV module output power and electrical efficiency of 18.90% and 22.98%, respectively. When the air is utilised for cooling the PV system, achieving a uniform airflow and determining the appropriate air source for the relatively small space under the PV array are important considerations. If the fan is utilised as a source of wind, what sort of fan should be used to ensure that the wind flow created can fully be channelled into the tight lower space between the PV module and the rooftop, given that the fan blades are significantly larger to generate more wind. All past researched cooling methods demonstrate that PV module performance can be enhanced by reducing the T_{cell} during operation. However, the majority of previous researches was conducted on prototypes developed on a modest scale. It is preferable to do research experiments on the existing *PV* system to evaluate and identify all elements and limits that exist when the cooling system is to be applied to the actual *PV* system, especially if installation on a building's roof is involved.

Therefore, the purpose of this research was to develop a temperature-based air-cooling system with variable fan speed to increase the efficiency of *PV* modules by lowering their operating temperature. The primary characteristics of this concept for an air-cooling system were proposed as follows:

- Uniform airflow
  DC cross-flow fan was utilized. Instead of creating a uniform and wide airflow system, the cross-flow fan was suitable for wide-width cooling.
- Energy saving concept
  The fan's speed depended on the temperature and allowed energy saving by preventing it from rotating continuously, limiting energy consumption

3. Methodology

The test was conducted under actual outdoor conditions on a six-year-old *PV* system in a tropical region (Kajang, Selangor, Malaysia). The irradiance, temperature, and electrical characteristics of the tested *PV* module was analysed and compared (with and without cooling). In addition, the design of the air-cooling system considered the space between the *PV* system and the rooftop, the area surrounding the *PV* system, ease of installation, and lighter weight to improve the performance of the *PV* module without modifying the existing *PV* system.

3.1 Concept of the cross-flow air-cooling system with speed regulation

The cooling system is comprised of an air-cooling system to decrease the T_{cell} by cooling the ventilation space beneath the installed *PV* array, thereby improving its efficiency, and utilising speed regulation to optimise energy. The primary objective was to produce uniform airflow beneath the *PV* array while lowering the T_{cell} using cross-flow fans. The fan was placed on the upper side of the solar array and a temperature sensor was attached to the back side of the *PV* module to detect changes on the T_{cell}, as shown in Figure 1. In this work, a minimum temperature has to be set based on the average T_{cell} per day at the site. When the T_{cell} exceeded the set minimum temperature, the microcontroller sent a signal to turn on the fan according to the *PWM* setting in the microcontroller. The fan then spun and the speed was dependent on the *PWM* settings. Any changes in

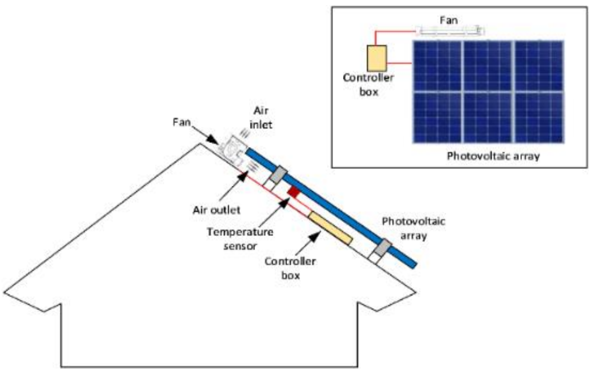

Fig 1. Proposed cooling system scheme

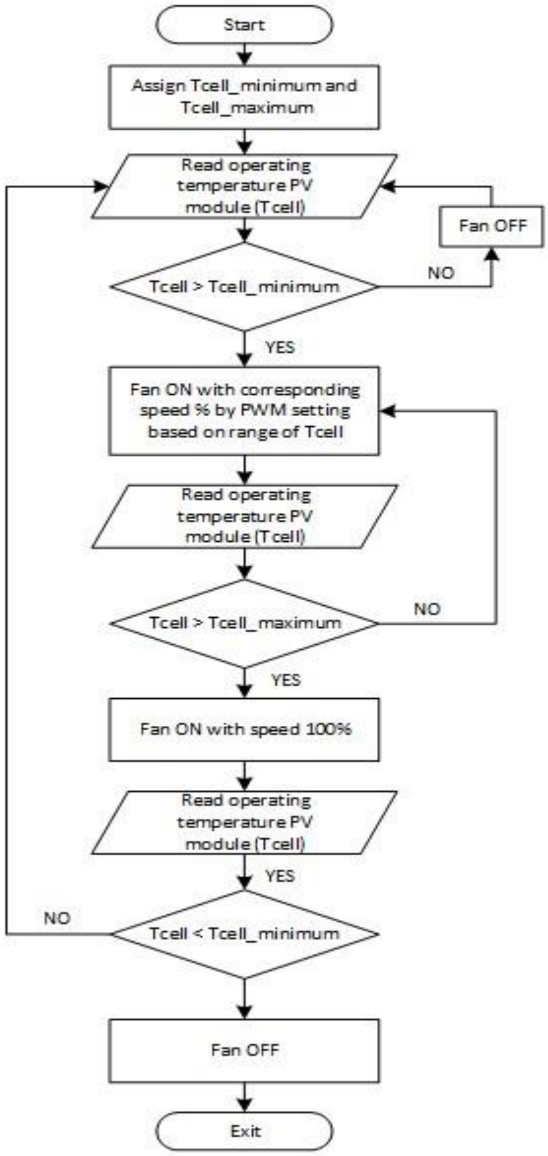

Fig 2. Flow chart of proposed controlling T_{cell} for air-cooling *PV* system

T_{cell} were detected and the fan speed adjusted accordingly. If the T_{cell} exceeded the maximum temperature, the fan continued to rotate at full speed. When the temperature dropped, the fan's speed decreased until it eventually stopped. The overall procedure for controlling T_{cell} is illustrated by the flow chart in Figure 2.

Table 1
Technical specifications for DC cross flow fan LWCD-401055M-30

Parameter	Specification
Dimension (mm)	A (1108), B (1065), C (1055)
Voltage (volt)	24
Current (ampere)	0.27
Speed (rpm)	2000
Pressure (Pa)	18
Airflow (m3/h)	290
Noise Db(A)	38

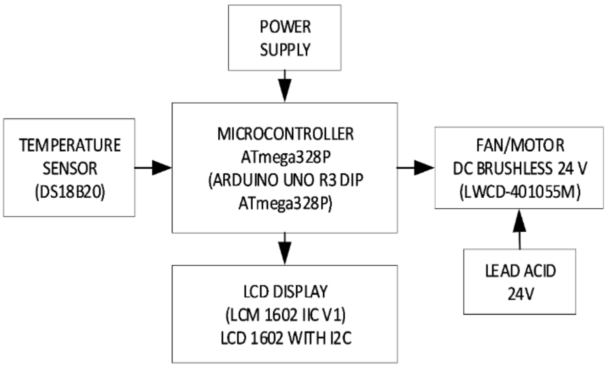

Fig 3. Simplified block diagram for a typical air-cooling system

Table 2
Specifications of the measuring instruments

Parameter	Range	Accuracy
Solar irradiance	0-1500 W/m2	+- 1.28%
Temperature	-55 C - 125°C	+- 0.5°C
DC voltage	0.1 - 330 V	+- 0.1%
DC current	0.1 - 20 A	+- 0.4 - 0.9%

3.2 DC cross-flow fan

To create a uniform airflow system, a DC cross-flow fan $LWCD - 401055M - 30$ with aluminium blade was utilized in this study. Table 1 contains its technical specifications. With less weight on the fan, this can solve the problem of heavy roof loads. To ensure safety features, it is essential to develop a system that is easy to install, lightweight and does not require a great deal of space when conducting studies on the actual PV system. Uniform air production is also important in this study, making this fan an option. The fan controller is a device designed to regulate the fan's operational time and speed at a predetermined temperature. The temperature sensor and fan are used as input and output controlled by the $ATMega328$ microcontroller to achieve this functionality. The waterproof version of the $DS18B20$ digital temperature sensor was used in this work. While the sensor can withstand temperatures up to 125^0C, the cable is PVC-coated and should be kept below 100^0C. The $DS18B20$ is compatible with systems between 3.0 and 5.5 V. Figure 3 shows a simplified block diagram for a typical air-cooling system used in this research. Table 2 displays the specifications of the instruments used in the experiment.

3.3 Location of experiment

Experimental tests were performed at the *GMi, Kajang Selangor Malaysia* at locations 2°55′59.2"N and 101°47′50.6"E. In general, the weather at *GMi* is humid, hot, and categorised by a tropical type of climate. It even has high atmospheric temperatures of above 40^0C, particularly between 11 a.m. to 3: 30 $p.m.$ (depending on the solar path for the day), which is a well-known challenge for the performance of PV systems. The polycrystalline PV system was installed on the zinc-type roof by a proper mounting structure and complied with Sustainable Energy Development Authority (SEDA) Malaysia requirements with a $40 - 50$ mm gap underneath the PV array. The $3kW$ grid-connected PV system utilised 12 pieces of 250 W polycrystalline PV module each, installed by $1 X 12$ configurations, which are one string with 12 modules per string. This system's performance was monitored by *Sunny SensorBox* via *Sunny Portal (www.sunnyportal.com)*. The *Sunny SensorBox* includes an integrated solar irradiance sensor and an external module temperature sensor, allowing for the comparison of irradiance levels and PV power based on the solar irradiance (W/m^2) measured by the sensor and the total amount of recorded power the PV system generates in a single day with a $15 -$ minute time interval.

3.3.1 Implementation of cross-flow air-cooling PV system

A prototype of the cross-flow air-cooling system was installed on a module of 250 W (1 module) of a 3 kW PV system. The PV system consisted of two 3 kW PV sub-array of poly-crystalline PVs, installed in an adjacent array configuration, making the position of both solar arrays the same as a single solar array, as shown in Figure 4. Daily, from sunrise to sunset, the PV system was not affected by any sort of shade. The performance of the PV module under standard test conditions (STC) (irradiance AM 1.5 1000 W/m^2, temperature 25^0C) is shown in Table 3.

The maximum power of the PV module decreased with the temperature by $-0.43\%/°C$, as stated in the temperature characteristics in Table 4. For the experimental tests, the cross-flow fan was placed on the upper side of the PV array. Experimental tests were done for only one module. The light metre $BH1750$ was positioned close to the same area so that the irradiance measured for analysis is more precise. Figure 5 depicts the location of the cross-flow fan and the light meter $BH1750$ within the PV system. The waterproof version of the digital temperature sensor $DS18B20$ was affixed to the back side of the solar module to detect temperature changes on the T_{cell}. This experiment was performed at the site for 12 continuous hours, from 7: 00 $a.m.$ to 7: 00 $p.m.$ Several days of experiments were conducted with and without the air-cooling system. The performance of a PV system is strongly reliant on the environment (Chandra S., 2018). The impact of irradiance, cell temperature, and windy conditions on PV systems is affected by geographical location as well as environmental and

Table 3
Technical specifications of the polycrystalline PV module under STC ($T_a = 25^0C, G = 100\ W/m^2$)

Parameter	Specification
Manufacturer	Canadian Solar
Model	CS6P-250P
Technology	Polycrystalline
Maximum power (W)	250
Maximum voltage (V)	30.1
Maximum current (A)	8.3
Open circuit voltage (V)	37.2
Short circuit current (A)	8.87
Number of cells	60 (6 X 10)
Dimension	1638 x 982 x 40 mm
Weight (kg)	18.5kg

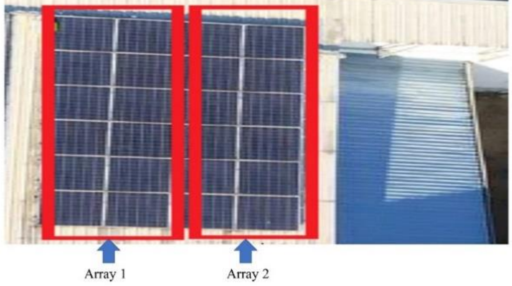

Fig 4. Two sub arrays installed in an adjacent array configuration

Table 4
Temperature characteristics for the *CS6P-250P Canadian Solar* PV module

Specification	Data
Temperature coefficient Pmax	-0.43%/C
Temperature coefficient Voc	-0.34%/C
Temperature coefficient Isc	0.065%/C
Nominal operating cell temperature (NOCT)	45+-2C

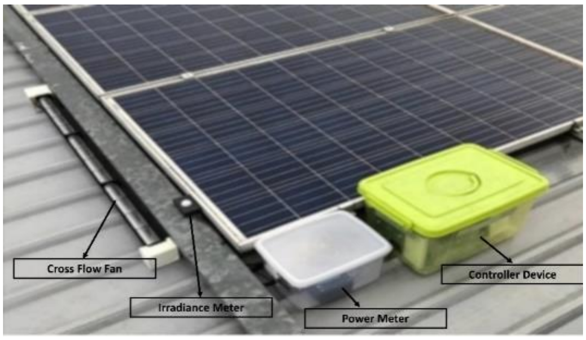

Fig 5. The location of the fan and the light meter $BH1750$ within the PV system

meteorological variables (M. R. Abdelkader, A. Al-Salaymeh, Z. Al-Hamamre, 2010). Malaysia is located in a low-wind zone (United Nations, 2016). Due to the low wind speed for the geographical region where the experiment was conducted, the model concluded that its influence was insignificant (Al-Bashir *et al*., 2020). Only ambient temperature and solar irradiance were examined among all important meteorological indicators for this investigation.

3.3. Ambient temperature, voltage and power at maximum point, and peak sun factor.

With an increase in solar irradiance, ambient temperature (T_{amb}) rose, increasing the temperature for both the front and rear PV modules. The surface of the PV module was more exposed to solar irradiance, and as a result, its surface temperature was greater. The transfer of heat occurs from hotter to cooler objects. Therefore, heat transfer occurred from the surface of the PV module to the back side, resulting in a backside T_{cell} that is higher than the T_{amb}. T_{amb} was calculated as (Reddy et al., 2015):

$$T_{amb} = T_{cell} - \left(\frac{NOCT-20}{800}\right) G_{amb} \qquad (1)$$

Where NOCT is nominal operating cell temperature (C^0) and G_{amb} is irradiance at that T_{amb} (W/m^2).

The maximum power point voltage (Vmp) and maximum power point power (Pmp) of a PV module are the voltage and power levels at which the module produces its highest output. These parameters are crucial for the effective operation of a PV module. The values of Vmp and Pmp are subject to variation based on the unique attributes of the PV module, including its design, technology, and environmental factors. When designing a PV system, it is important to consider a certain value that assists in identifying the suitable arrangement of PV modules for achieving the specified power output. This study aims to measure and compare these parameters values under real operating conditions, referred to V_{mp_exp} and P_{mp_exp}, with the predicted calculated values, referred to as V_{mp_calc} and P_{mp_calc}.

The maximum power point voltage of the PV module was calculated (V_{mp_calc}) as follows:

$$V_{mp\_calc} = V_{mp\_stc}\, X\, [1 + \left(\frac{\gamma_{V_{mp}}}{100}\right)(T_{cell} - T_{stc})] \qquad (2)$$

where V_{mp_stc} is voltage at maximum power point at STC and $\gamma_{V_{mp}}$is temperature coefficient for voltage at maximum power point.
The maximum power point power of the PV module was calculated (P_{mp_calc}) as follows:

$$P_{mp\_roc\_calc} = P_{mp_{stc}}\, X\, [1 + \left(\frac{\gamma_{P_{mp}}}{100}\right)(T_{cell} - T_{stc})] \qquad (3)$$

where P_{mp_stc} is power at STC (Watt) $\gamma_{P_{mp}}$is temperature coefficient for power at maximum power point.

On the same system, experiments were conducted on different days with and without the air-cooling system. Since external factors such as weather and solar irradiance cannot be controlled, it is essential to compare the output before and after installation of the air-cooling system based on a single factor. In many cases, it may be required to estimate the instantaneous outputs of the PV module or array under real operating conditions. In ROC situations, solar irradiance and temperature are instantaneous values that have an immediate effect on PV module outputs. Moreover, solar irradiance fluctuates rapidly, and the output of the PV module varies in tandem with solar irradiance. Consequently, a concept known as the PSF was used to determine the expected instantaneous output as follows:

$$PSF = \frac{G_{array\_plane}}{1{,}000\ Wm^{-2}} \qquad (4)$$

Where PSF is Peak Sun Faktor (dimensionless) and G_{array_plane} is solar irradiance in array plane (Wm^{-2})

4. Result and discussion

A reference measurement was carried out for a typical day on $April\ 14, 2021$ from the GMi-monitoring system at sunny portal. Figure 6 depicts the $15-minutes$ interval recording from $Sunny\ Box$ for measured irradiance and T_{cell}, without a cooling system between $12{:}15\ a.m.$ and $11{:}45\ p.m$ for the correspond

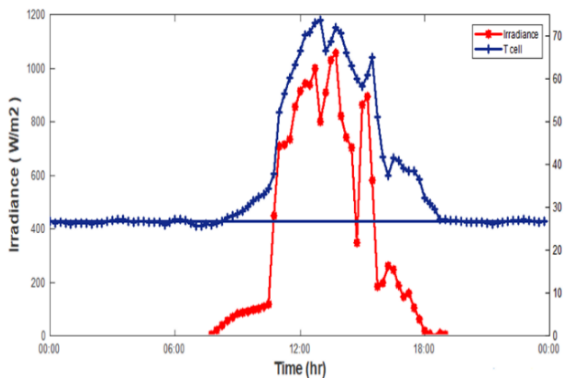

Fig 6. Solar irradiance and T_{cell} for a typical day from GMi PV system monitoring.

day. From the chart, the maximum T_{cell} was 73.69^0C at $1:00\,pm$, with solar irradiance $801.1W/m^2$. T_{cell} varied from 26^0C up to 63^0C in the morning, while the noon T_{cell} can exceed 73^0C. Solar irradiance reached up to $1113W/m^2$ for the day. Figure 7 illustrates the experimental data obtained for the observed solar irradiance, T_{cell} , and T_{amb} from the *PV* system on normal days, both before and after the air-cooling *PV* system was put in place. The percentage difference between the experimental and the measurements data from the *GMi*-monitoring system is negligible, at approximately 0.8 %, so the experiment data in Figure 7 is applicable. This small disparity is attributed to the information on the global horizontal irradiance (*GHI*) daily intra-variability that can be obtained by characterizing the solar irradiance at the study site (Al-Kayiem & Mohammad, 2019) such as, the daily clearness coefficient, considering various cloud cover (Urrego-Ortiz et al., 2019) (Urrego-Ortiz et al., 2019), as well as the sun's path, particularly in tropical climate regions.

According to the chart in Figure 7, the highest temperature of the *PV* system before employing air cooling system was 72.88^0C at 1:08 pm, with an average solar irradiance of $738.64\ W/m^2$. The temperature of T_{cell} ranged from 24^0C to 65^0C in the morning, with the possibility of exceeding 72^0C around midday. The solar irradiance reached a maximum of $1098.29W/m^2$ on the experimental day prior to implementing the air-cooling PV system. Consequently, the greatest T_{cell} value did not necessarily coincide with the peak solar irradiance. It is probable that the maximum solar irradiance occurred in a very brief period of time and did not have sufficient time to influence the T_{cell} value. This is also demonstrated by the data collected by the existing system at the study site via Sunny Web Portal.

4.1. Cooling effect on T_{cell}

An experiment was conducted by attaching an air-cooling system to the existing real *PV* system at *GMi* and the results were recorded continuously from $7:00\ am$ to $7:00\ pm$. From the graphs in Figure 7, it appears that T_{cell} is higher than T_{amb}. It is essential to ensure that the backside of the *PV* module is cooled to reduce the T_{cell}. By providing uniformed air conduction underneath the *PV* module, this study ensured that cold air floated, preventing the trapping of hot air underneath the module. As already observed in Figure 7, T_{cell} increased as solar irradiance increased. Figure 7 demonstrates that the system with an installed air- cooling system experienced a slower rise in temperature after 30^0C compared to the system without a cooling system. This is due to the fact that after the installation of the cooling system when the T_{cell} exceeded 30^0C, the fan began to rotate at a speed of 4% and changed significantly with the changes in the T_{cell}. Consequently, although solar irradiance increased, the T_{cell} did not continue to increase at the same rate. The T_{cell} continued to rise, but at a slower rate than when no cooling system was installed. Nonetheless, it should be noted that the ratio between the amount of solar irradiance and the duration of time a *PV* module receives solar irradiance plays a significant role. When the amount and duration of solar irradiance received is high and relatively prolonged, the T_{cell} rises more rapidly. Alternatively, if the amount of solar irradiance received is high but over a brief period, the *PV* module change will still occur, but it will take longer and the rate of T_{cell} increase will be slower. This is because the air conduction factor produced by the installed cooling system has pushed out the hot air trapped beneath the *PV* module, which has the potential to raise the T_{cell}. After implementing the air-cooling *PV* system, Figure 7 shows that morning temperature varied up to 54.13^0C while the midday

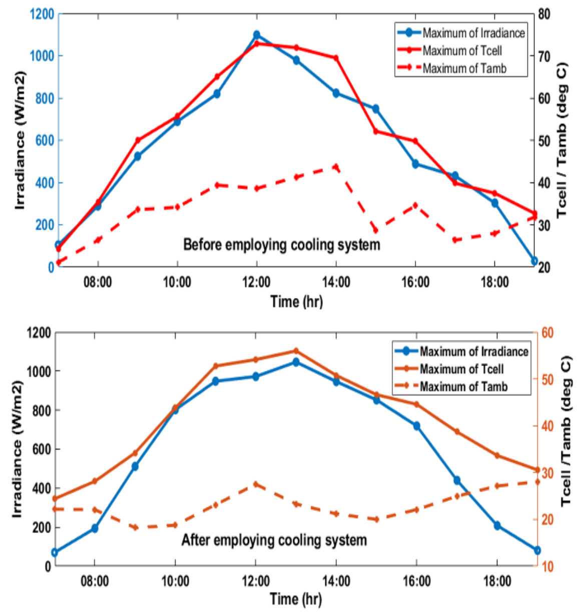

Fig 7. Graph depicting the relationship between maximum T_{cell} and T_{amb} values and the corresponding measured solar irradiance at the *PV* system during the respective days before and after employing an air-cooling *PV* system.

temperature did not exceed 55.98^0C. The maximum T_{cell} was 55.98^0C between $1.00\ to\ 2.00\ p.m$, with the maximum solar irradiance $1046.49\ W/m^2$. For average frequently solar irradiance $800\ W/m^2$, the average maximum T_{cell} was 70^0C before employing air-cooling *PV* system while 49.5^0C after applying an air-cooling *PV* system. Compared to the previous

Table 5
Total average *PSF* received per day for respective experimental days, with average energy consumed by the fan for the cooling system

Time	Day 1 (without cooling system)	Day 2 (with cooling system)	
	Average PSF	Average PSF	Average Energy consumed by fan (Wh)
7:00 AM	0.03	0.04	0
8:00 AM	0.17	0.11	0
9:00 AM	0.38	0.4	2.52
10:00 AM	0.53	0.53	5.18
11:00 AM	0.68	0.75	5.95
12:00 PM	0.74	0.6	5.98
1:00 PM	0.68	0.56	6.02
2:00 PM	0.72	0.7	5.63
3:00 PM	0.55	0.61	5.55
4:00 PM	0.36	0.51	5.41
5:00 PM	0.37	0.37	5.15
6:00 PM	0.13	0.15	4.51
7:00 PM	0.03	0.08	0
TOTAL	**5.38**	**5.4**	**51.89**

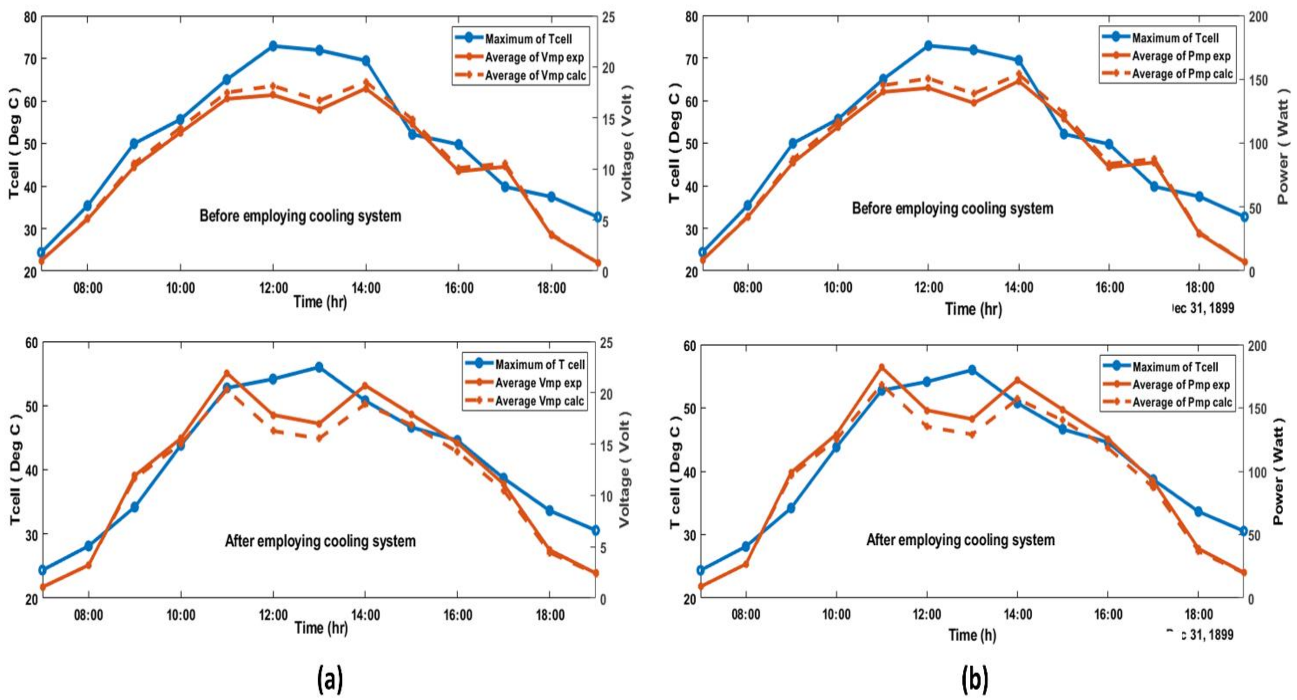

Fig 8. Experimental and calculated values before and after employing an air-cooling PV system based on corresponding T_{cell} for respective testing day: (a) voltage and (b) power

condition without the cooling system, where the temperature of T_{cell} varied from 24^0C to 65^0C in the morning and had the potential to surpass 72^0C around midday, it is evident that the implementation of the recommended cooling system has effectively lowered the T_{cell} value.

The comparison is based on the two closest days with and without an air-cooling PV system when weather conditions were relatively similar, but it should be emphasised that weather conditions are uncontrollable. The choice of days to compare is important to make sure that the analysis of data is more accurate and useful. Table 5 shows data on solar irradiance received by total PSF per day for both before and after implementing the cooling system. The daily quantity of irradiance received is independent of the cooling system being evaluated but is contingent upon the meteorological conditions of the day. To ensure accuracy, it is important to measure the irradiance levels on both days while conducting the test, either before or after the installation of the cooling system. The table shows that the total average PSF for day 1, where the measured parameters were taken before employing the cooling system was 5.38, while on day 2, when the experiment was conducted with the cooling system in place, the total average PSF was 5.4. This demonstrates that despite the experiments being conducted on separate days, the average amount of irradiance received throughout both days of the experiment was about similar and relevant.

4.2. Cooling effect on the output voltage and power

With an increase in T_{cell}, the initial rise in irradiance led to a rise in voltage. The same holds for the current, which is directly proportional to solar irradiance. However, when the temperature further climbed, an increase in irradiance resulted in a decrease in voltage. the increase in irradiance will initially result in the addition of T_{cell} and will increase the voltage value but when T_{cell} achieved over 25^0C, the voltage will start to decrease depending on how much the PV module affected by temperature coefficient. The temperature coefficient, γ, at the maximum power point refers to the impact of thermal expansion on the voltage, power and current of the PV module. In this investigation, the temperature coefficient for voltage was determined to be -0.43%/°C. The same principle applies to the power that is generated. The prolonged voltage dips led to a substantial power loss that has to be resolved. Figure 8 illustrates the graphs showing the changes in voltage (V_{mp_exp} and V_{mp_calc}) and power (P_{mp_exp} and P_{mp_calc}) before and after implementing the cooling PV system during experimental circumstances and expected calculations. Based on the comparison between V_{mp_exp} and V_{mp_calc}, as well as P_{mp_exp} and P_{mp_calc} in Figure 8, it was found that the measured values of V_{mp_exp} and P_{mp_exp} were lower than the calculated values before employing the cooling PV system. This difference was particularly noticeable in Figure 8, when the T_{cell} value exceeded $50°C$, which happened between $10.00\, a.m.$ and $3.00\, p.m.$ This demonstrates that the inclusion of T_{cell} will have an impact on the performance of V_{mp_exp} and P_{mp_exp}, which is contingent upon the current T_cell, PSF, and γ being taken into consideration.

Figure 9 shows the total average voltage and power produced by the PV module compared to the total average voltage and power expected to be produced. Since the experiment was done on two different days with almost the same irradiance level value, this study has made a comparison of the total values of voltage and power produced during the experiment, which are V_{mp_exp} and P_{mp_exp}, to the values expected through calculation, which are V_{mp_calc} and P_{mp_calc} before and after employing the cooling system. This is to get a more accurate comparison, even though the wind factor is neglected in this study based on the metrology of the experimental area. Prior to implementing the air-cooling PV system, the testing findings indicated that a rise in T_{cell} led to a drop-in voltage and power values by 3.75% and 3.73% respectively, compared to the estimated value, despite an

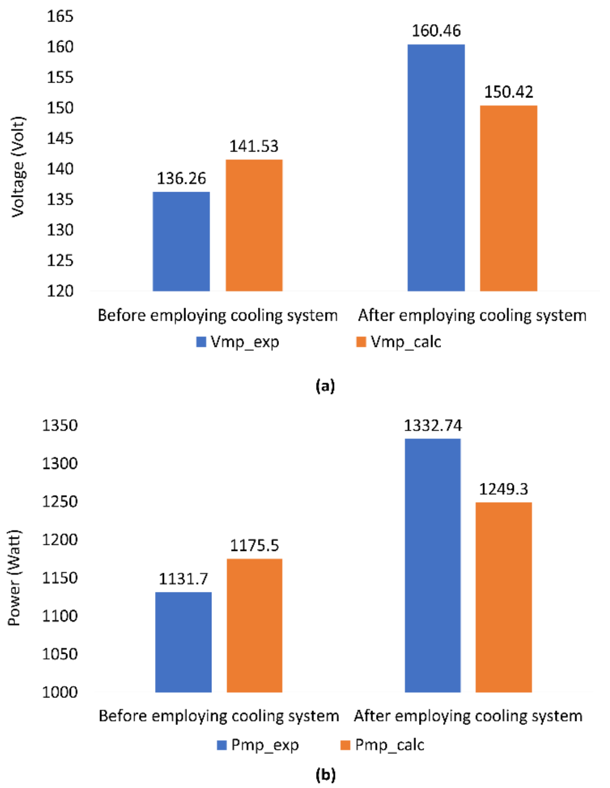

Fig 9. Total average voltage and power at maximum power point at real operating condition and expected value: (a) voltage and (b) power

increase in solar irradiance. In addition to successfully extending the time it takes for the temperature of a T_{cell} to rise, the installation of an air-cooling PV system can also control the voltage drop that occurs when the temperature rises to ridiculous levels. After implemented the air-cooling PV system, V_{mp_exp} and P_{mp_exp} were higher than the calculation, particularly when the T_{cell} value was above 50^0C, which occurred between 11.00 $a.m.$ and 3.00 $p.m$, as shown in Figure 8. The gains from 0.5 V to 1.81V and 0.43 W to 15.03 W for voltage and power respectively. The percentages varied from 2.16% up to 8.76% and 2.2% up to 9.6% for voltage and power. When T_{cell} was above 30^0C at 9.00 a.m. and over, the measured V_{mp_exp} and P_{mp_exp} started higher than V_{mp_calc} and P_{mp_calc}. V_{mp_exp} and $P_{mp\_roc\_exp}$ continued to rise as the increase in irradiance, but when T_{cell} started higher than 50^0C, V_{mp_exp} and P_{mp_exp} began to decline. However, the V_{mp_exp} and P_{mp_exp} readings continued to exceed the calculation value. When T_{cell} began to decrease, the V_{mp_exp} and P_{mp_exp} started to increase with an increasing irradiance. After 5.00 $p.m.$, $Tcell$ started to drop below 30^0C and the V_{mp_exp} and P_{mp_exp} approached the value of calculation as the irradiance began to decrease and the afternoon weather was cloudier and windier at the experiment area. From Figure 9, the total average voltage and power were 10.05 V and 83.44 W, higher than the calculated value which was 6.68% energy efficient. The results of the proposed air-cooling PV system were compared, as shown in Table 6, with those of Lebbi *et al.* (Lebbi *et al.*, 2021), A.E. Kabeel *et al.* (Kabeel *et al.*, 2019), Arcuri *et al.* (Arcuri *et al.*, 2014), Mazón- Hernández *et al.* (Mazón-Hernández *et al.*, 2013), and Kidegho *et al.* (Kidegho *et al.*, 2021). All PV modules were compared based on the proportion of power performance under which they operated. The output power and efficiency of PV modules increased when cooling systems were utilised. However, there are no exhaustive comparisons of the power rating per module used in the research system in the literature. The current study involved a 6.48 W power rating for the proposed system, utilising a 250 Wp PV module measuring $1638\ x\ 980\ x\ 40\ mm$, with an average net improvement in output power of 12.9%, which is nearly 9% higher than what Lebbi *et al.* (Lebbi *et al.*, 2021) achieved.

This proposed system has one of the two lowest power ratings per module at 2.6%. Another lowest was found by Arcuri *et al.* (Arcuri *et al.*, 2014) also with 2.6%. The system introduced by Arcuri *et al.* (Arcuri *et al.*, 2014) had a power rating of 3.6 W and used a $1041\ x\ 989\ x\ 35\ mm$, 140 Wp PV module. Although the power rating system by Arcuri *et al.*(Arcuri *et al.*, 2014) is much lower than the proposed system, the power of used PV module cannot match with the proposed system, which is much larger and only produced gain in power by 0.19% compared to 12.9% net for the proposed one. A.E. Kabeel *et al.* (Kabeel *et al.*, 2019) achieved the biggest net improvement in output power but came with the highest power rating, 15 W for the introduced methtod, using 130 Wp PV module and a lower size of $1482\ x\ 672\ x\ 35\ mm$ than the one proposed. The method by A.E. Kabeel *et al.* (Kabeel *et al.*, 2019) had the highest percentage power rating per module at 11.5%. In terms of power rating per system and per PV module, the proposed air-cooling PV system outperforms both Arcuri *et al.* (Arcuri *et al.,* 2014) and A.E. Kabeel *et al.* (Kabeel *et al.,* 2019). This is due to the peak power of PV module and size employed were significantly larger than those used by Arcuri *et al.* (Arcuri *et al.*, 2014) and A.E. Kabeel *et al* (Kabeel *et al.*, 2019). The superiority of the proposed air-cooling PV system as compared to Lebbi *et al.*(Lebbi *et al.*, 2021), Mazón-Hernández *et al.* (Mazón-Hernández et al., 2013), and Kidegho *et al.*(Kidegho *et al.*, 2021) is evident from Table 6. The passive cooling approach utilised by Kidegho *et al.*(Kidegho *et al.*, 2021) had zero power rating and was applied to 13 Wp PV modules with dimensions of $325\ x\ 325\ x\ 20\ mm$ where they achieved PV power production by 1.8%. The experiment was conducted on the smallest PV module as shown in Table 6 and consumed no power but produced lower output power. Compared to the proposed air-cooling PV system, it is preferable to adopt a system that is more power-efficient, such as the one in the proposed system, which has a low power rating per module and can provide a relatively large power output. Consequently, it is essential to remember that the cooling temperature range plays a crucial role in preventing energy waste. It is good to prevent the consumption of more energy for air-cooling systems than can be generated. Consequently, it is essential to remember that the cooling temperature range plays a crucial role in preventing energy waste. It is good to prevent the consumption of more energy for air-cooling systems than can be generated. Therefore, it is essential to regulate the correct temperature ranges so that the desired temperature can reduce or prevent voltage drops. Since a relatively large heat transfer occurs in the roof area due to uncontrollable external factors, it is impossible to achieve a temperature that is too low or to approach the STC for the rooftop PV system.

4.3. Cooling effect based on peak sun factor (PSF)

Estimating the instantaneous output of a PV module or array under real operating conditions is crucial in certain situations. This is due to the fact that irradiance and temperature are instantaneous variables that have an immediate impact on the output of the PV module. This study utilised PSF to calculate the average power output for each received PSF. According to Table 5, the total PSF attained the day before the cooling

Table 6
Comparison of past studies including current investigation and findings

No.	References	Analysis type and System Design	Type of Cooling	Method	PV Specification	Finding	Rating Power of Cooling System (fan/pump)	Operational time & Rating Power per Module	Energy consumption for 8 hrs
1	Lebbi, 2021	Experimental / Model	Active cooling	Forced air circulation backside of PV module while its front flowing water	90 W 1200 x 550 x 30 mm	Average electrical efficiency of 3.7% for hybrid system	4.6 W	8 hrs 5.1%	46 Wh
2	A.E. Kabeel, 2019	Experimental / Model	Active cooling	Forced air technologies together in the presence of reflectors	130 W 1482 × 676 × 35 mm	Average 22.42% net output power	15 W	10 hrs 11.5%	150 Wh
3	Arcuri 2014	Experimental / Model and simulation	Active cooling	Force air underneath PV module using helical fan attached to air duct covering the entire back surface of the PV module	140 W 1041 x 991 x 35 mm	Gain0.19% output power and 5% per year	3.6 W	12 hrs 2.6%	36 Wh
4	Mazón-Hernández, 2013	Experimental / Model	Active cooling	Force air underneath PV module using centrifugal fan attached to air duct	240 W 1956 × 992 × 50 mm	Gain 7.5% output power	NA	8 hrs	NA
5	Kidegho, 2021	Experimental / Model and simulation	Passive cooling	Thermal interface materials (TIM) under air environments with aluminium honeycomb cooling panels as the cooling contact medium	13 W 325 × 325 × 20 mm	PV module power output increased by 1.8%	NA	5 hrs	NA
6	Proposed system	Experimental / Existing PV system on steel rooftop	Active cooling	Force air using cross flow fan attached top between PV module and roof top	250 W 1638 x 982 x 40 mm	Gain 13.18% average net output power	6.48 W	12 hrs 2.6%	51.89 Wh

system was installed was 5375, which is equivalent to 5.38 average peak sun hours (PSH) where the PV module received $1000W/m^2$. The entire daily power output for this was $1131.70\ W$, as seen in Figure 8. Under real-world operating circumstances, the average instantaneous power output of PV

modules before employing the cooling system was 210.35 W per PSF at $1000W/m^2$ of solar irradiance.

The amount of total PSF achieved on the day where the air-cooling PV system was applied was 5402, equal to 5.40 for PSH. The total power generated by the PV module on that day was 1332.74 W and the average output power per PSF at 1000 W/m^2 of solar irradiance was 246.80 W. Compared to the before and after applying the studied air-cooling PV system, the anticipated instantaneous average power output of PV modules increased by 17.3%, which is equal to 36.45W. Although numerous researches have been conducted to establish the efficacy of PV cooling systems, the majority of them were conducted using simulations. Six previous experiment-based research works with credible findings were chosen to further validate against the proposed air-cooling PV system. As can be seen in Table 6, the proposed air-cooling PV system achieved a large net gain on average power, while using only a fraction of the power throughout the course of the day. Even though the proposed air-cooling PV system was tested at an already-existing roof-top PV system, the results were still superior to earlier experiment-based research on a single PV module. The achievements show that the proposed air-cooling system with an innovative cross-flow fan can significantly boost the efficiency of modules in comparison to the previous research system. Even though there is zero power loss while using the passive cooling approach, the increase in power output of the module can't be matched by the proposed active cooling method. The effectiveness and capability of the proposed air-cooling system proved successful, as greater energy was produced than was consumed during cooling processes.

5. Conclusion

In this study, an air-cooling system for an existing polycrystalline PV system was developed and experimentally investigated under tropical climate conditions. The air-cooling system relied on a cross-flow fan that produced a uniform airflow between the rear of the PV module and the roof. This temperature-based system with variable fan speed and user-friendly installation was placed directly to the side of the existing PV system without modification. Based on the results obtained, some conclusions have been drawn. T_{cell} is greater than T_{amb}; consequently, wind intake from an open-air or ambient surroundings PV system can provide wind with a lower temperature than wind discovered between PV modules and rooftop, thereby lowering T_{cell} by expelling the hot wind trapped in the space beneath the PV array by using a cross-flow fan. With the support of the utilised air-cooling PV system, a maximum temperature of T_{cell} decreased with maximum reference T_{cell} ranged from 24.37^0C to 72.88^0C. In contrast, the maximum cooled T_{cell} ranged from 24.37^0C to 55.98^0C. Due to the temperature reduction afforded by the employed air-cooling method, the PV module output power and conversion efficiency were significantly improved. The anticipated instantaneous power output of PV modules increased by 17.3%, from 210.35 to 246.80 W per PSF. 13.18% increase in average net output power with 6.68% energy efficiency. Energy consumption for the proposed air-cooling PV system was 51.89 Wh per day, which is only 3.89% per PV module. While the peak power of PV module and size employed were significantly larger, the proposed air-cooling PV system outperforms previous research with the lowest power rating per module, 2.6% but achieved high net average power improvement and it really attained 6.32 W, which is 2.53% per PV module. Based on the experimental findings, it is possible to conclude that the proposed air-cooling system enhanced the temperature regulation and performance of the PV module significantly. This is because the experiment was conducted on an existing PV system on a zinc-type roof, where zinc is a conductor that allows for a substantial heat transfer under high irradiance. This system is also user-friendly, silent, has a low initial investment cost, and is lighter. In terms of future research, this air-cooling technology must be investigated further, considering other variables that may affect the cooling efficiency, such as wind speed, roof type, and fan blade.

Acknowledgments

The authors would like to acknowledge the Ministry of Higher Education for financial support via Fundamental Research Grant Scheme FRGS/1/2019/TK07/UPM/02/2. Also, a special thanks to Advanced Lightning Power Energy Research (ALPER), Universiti Putra Malaysia and the German Malaysian Institute for providing lab, equipment, and an award to the project's primary author.

Author Contributions: Rozita Mustafa: Conceptualization, Methodology, Investigation, Validation, Visualization, Writing - original draft. Slimane Mohd Amran Mohd Radzi: Supervision, Project administration, Validation, Writing - review & editing. Hashim Hizam: Investigation, Validation. Azura Che Soh: Visualization, Formal analysis, Software.

Funding: The author(s) received no financial support for the research, authorship, and/or publication of this article.

Conflicts of Interest: The authors declare no conflict of interest.

References

Abdulmunem, A. R., Mohd Samin, P., Abdul Rahman, H., Hussien, H. A., Izmi Mazali, I., & Ghazali, H. (2021). Numerical and experimental analysis of the tilt angle's effects on the characteristics of the melting process of PCM-based as PV cell's backside heat sink. Renewable Energy, 173, 520–530. https://doi.org/10.1016/j.renene.2021.04.014

Adaramola, M. S. (2015). Techno-economic analysis of a 2.1 kW rooftop photovoltaic-grid-tied system based on actual performance. Energy Conversion and Management, 101, 85–93. https://doi.org/10.1016/j.enconman.2015.05.038

Al-Bashir, A., Al-Dweri, M., Al-Ghandoor, A., Hammad, B., & Al-Kouz, W. (2020). ANALYSIS OF EFFECTS OF SOLAR IRRADIANCE, CELL TEMPERATURE AND WIND SPEED ON PHOTOVOLTAIC SYSTEMS PERFORMANCE. International Journal of Energy Economics and Policy, 10(1), 353–359. https://doi.org/10.32479/ijeep.8591

Al-Kayiem, H., & Mohammad, S. (2019). Potential of Renewable Energy Resources with an Emphasis on Solar Power in Iraq: An Outlook. Resources, 8(1), 42. https://doi.org/10.3390/resources8010042

Amelia, A. R., Irwan, Y. M., Irwanto, M., Leow, W. Z., Gomesh, N., Safwati, I., & Anuar, M. A. M. (2016). Cooling on photovoltaic panel using forced air convection induced by DC fan. International Journal of Electrical and Computer Engineering, 6(2), 526–534. https://doi.org/10.11591/ijece.v6i1.9118

Arcuri, N., Reda, F., & De Simone, M. (2014). Energy and thermo-fluid-dynamics evaluations of photovoltaic panels cooled by water and air. Solar Energy, 105, 147–156. https://doi.org/10.1016/j.solener.2014.03.034

Castanheira, A. F. A., Fernandes, J. F. P., & Branco, P. J. C. (2018). Demonstration project of a cooling system for existing PV power plants in Portugal. Applied Energy, 211, 1297–1307. https://doi.org/10.1016/j.apenergy.2017.11.086

Chandra S., A. S. and D. S. C. (2018). Effect of Ambient Temperature and Wind Speed on Performance Ratio of Polycrystalline Solar

Photovoltaic Module: an Experimental Analysis. International Energy Journal, 18, 171 – 180. https://www.researchgate.net/publication/325952592_Effect_of_ambient_temperature_and_wind_speed_on_performance_ratio_of_polycrystalline_solar_photovoltaic_module_An_experimental_analysis

Dida, M., Boughali, S., Bechki, D., & Bouguettaia, H. (2021). Experimental investigation of a passive cooling system for photovoltaic modules efficiency improvement in hot and arid regions. Energy Conversion and Management, 243. https://doi.org/10.1016/j.enconman.2021.114328

Elbreki, A. M., Sopian, K., Fazlizan, A., & Ibrahim, A. (2020). An innovative technique of passive cooling PV module using lapping fins and planner reflector. Case Studies in Thermal Engineering, 19, 100607. https://doi.org/10.1016/j.csite.2020.100607

Elminshawy, N. A. S., El Ghandour, M., Gad, H. M., El-Damhogi, D. G., El-Nahhas, K., & Addas, M. F. (2019). The performance of a buried heat exchanger system for PV panel cooling under elevated air temperatures. Geothermics, 82, 7–15. https://doi.org/10.1016/j.geothermics.2019.05.012

Elminshawy, N. A. S., Mohamed, A. M. I., Morad, K., Elhenawy, Y., & Alrobaian, A. A. (2019). Performance of PV panel coupled with geothermal air cooling system subjected to hot climatic. Applied Thermal Engineering, 148, 1–9. https://doi.org/10.1016/j.applthermaleng.2018.11.027

Fatoni, E. K. A., Taqwa, A., & Kusumanto, R. (2019). Solar Panel Performance Improvement using Heatsink Fan as the Cooling Effect. Journal of Physics: Conference Series, 1167(1). https://doi.org/10.1088/1742-6596/1167/1/012031

Gomaa, M. R., Hammad, W., Al-Dhaifallah, M., & Rezk, H. (2020). Performance enhancement of grid-tied PV system through proposed design cooling techniques: An experimental study and comparative analysis. Solar Energy, 211, 1110–1127. https://doi.org/10.1016/j.solener.2020.10.062

Grubišić Čabo, F., Nižetić, S., Giama, E., & Papadopoulos, A. (2020). Techno-economic and environmental evaluation of passive cooled photovoltaic systems in Mediterranean climate conditions. Applied Thermal Engineering, 169, 114947. https://doi.org/10.1016/j.applthermaleng.2020.114947

Haidar, Z. A., Orfi, J., & Kaneesamkandi, Z. (2018). Experimental investigation of evaporative cooling for enhancing photovoltaic panels efficiency. Results in Physics, 11, 690–697. https://doi.org/10.1016/j.rinp.2018.10.016

Hamzat, A. K., Sahin, A. Z., Omisanya, M. I., & Alhems, L. M. (2021). Advances in PV and PVT cooling technologies: A review. Sustainable Energy Technologies and Assessments, 47, 101360. https://doi.org/10.1016/j.seta.2021.101360

Hernandez-Perez, J. G., Carrillo, J. G., Bassam, A., Flota-Banuelos, M., & Patino-Lopez, L. D. (2021). Thermal performance of a discontinuous finned heatsink profile for PV passive cooling. Applied Thermal Engineering, 184, 116238. https://doi.org/10.1016/j.applthermaleng.2020.116238

Hussien, H. A., Numan, A. H., & Abdulmunem, A. R. (2015). Improving of the photovoltaic / thermal system performance using water cooling technique. IOP Conference Series: Materials Science and Engineering, 78(1). https://doi.org/10.1088/1757-899X/78/1/012020

Idoko, L., Anaya-Lara, O., & McDonald, A. (2018). Enhancing PV modules efficiency and power output using multi-concept cooling technique. Energy Reports, 4, 357–369. https://doi.org/10.1016/j.egyr.2018.05.004

Jie Ji, Jian-Ping Lu, Tin-Tai Chow, Wei He, G. P. (2007). A sensitivity study of a hybrid photovoltaic/thermal water-heating system with natural circulation. Applied Energy, 84, 222–237. https://doi.org/10.1016/j.apenergy.2006.04.009

Joseph Paul, S., Kumar, U., & Jain, S. (2021). Photovoltaic cells cooling techniques for energy efficiency optimization. Materials Today: Proceedings, 46, 5458–5463. https://doi.org/10.1016/j.matpr.2020.09.197

Kabeel, A. E., Abdelgaied, M., & Sathyamurthy, R. (2019). A comprehensive investigation of the optimization cooling technique for improving the performance of PV module with reflectors under Egyptian conditions. Solar Energy, 186, 257–263. https://doi.org/10.1016/j.solener.2019.05.019

Kaewchoothong, N., Sukato, T., Narato, P., & Nuntadusit, C. (2021). Flow and heat transfer characteristics on thermal performance inside the parallel flow channel with alternative ribs based on photovoltaic/thermal (PV/T) system. Applied Thermal Engineering, 185, 116237. https://doi.org/10.1016/j.applthermaleng.2020.116237

Kidegho, G., Njoka, F., Muriithi, C., & Kinyua, R. (2021). Evaluation of thermal interface materials in mediating PV cell temperature mismatch in PV–TEG power generation. Energy Reports, 7, 1636–1650. https://doi.org/10.1016/j.egyr.2021.03.015

Lebbi, M., Touafek, K., Benchatti, A., Boutina, L., Khelifa, A., Baissi, M. T., & Hassani, S. (2021). Energy performance improvement of a new hybrid PV/T Bi-fluid system using active cooling and self-cleaning: Experimental study. Applied Thermal Engineering, 182, 116033. https://doi.org/10.1016/j.applthermaleng.2020.116033

Lee, S., Iyengar, S., Feng, M., Shenoy, P., & Maji, S. (2019). Deeproof: A data-driven approach for solar potential estimation using rooop imagery. Proceedings of the ACM SIGKDD International Conference on Knowledge Discovery and Data Mining, 2105–2113. https://doi.org/10.1145/3292500.3330741

M. R. Abdelkader, A. Al-Salaymeh, Z. Al-Hamamre, F. S. (2010). A comparative Analysis of the Performance of Monocrystalline and Multiycrystalline PV Cells in Semi Arid Climate Conditions: the Case of Jordan. Jordan Journal of Mechanical and Industrial Engineering. All Rights Reserved, 4(5), 543–552.

Mattei, M., Notton, G., Cristofari, C., Muselli, M., & Poggi, P. (2006). Calculation of the polycrystalline PV module temperature using a simple method of energy balance. Renewable Energy, 31(4), 553–567. https://doi.org/10.1016/j.renene.2005.03.010

Mazón-Hernández, R., García-Cascales, J. R., Vera-García, F., Káiser, A. S., & Zamora, B. (2013). Improving the Electrical Parameters of a Photovoltaic Panel by Means of an Induced or Forced Air Stream. International Journal of Photoenergy, 2013, 1–10. https://doi.org/10.1155/2013/830968

Moharram, K. A., Abd-Elhady, M. S., Kandil, H. A., & El-Sherif, H. (2013). Enhancing the performance of photovoltaic panels by water cooling. Ain Shams Engineering Journal, 4(4), 869–877. https://doi.org/10.1016/j.asej.2013.03.005

Pandey, O. P., Dung, V. V. D., Mishra, P., & Kumar, R. (2022). Simulating rooftop solar arrays with varying design parameters to study effect of mutual shading. Energy for Sustainable Development, 68, 425–440. https://doi.org/10.1016/j.esd.2022.04.010

Rawat, R., Kaushik, S. C., & Lamba, R. (2016). A review on modeling, design methodology and size optimization of photovoltaic based water pumping, standalone and grid connected system. Renewable and Sustainable Energy Reviews, 57, 1506–1519. https://doi.org/10.1016/j.rser.2015.12.228

Reddy, S. R., Ebadian, M. A., & Lin, C.-X. (2015). A review of PV–T systems: Thermal management and efficiency with single phase cooling. International Journal of Heat and Mass Transfer, 91, 861–871. https://doi.org/10.1016/j.ijheatmasstransfer.2015.07.134

Sethiya, A. (2021). Cooling material for solar PV module to improve the generation efficiency. Materials Today: Proceedings, 47, 7064–7066. https://doi.org/10.1016/j.matpr.2021.06.122

Sharma, R., Singh, S., Mehra, K. S., & Kumar, R. (2021). Performance enhancement of solar photovoltaic system using different cooling techniques. Materials Today: Proceedings, 46, 11023–11028. https://doi.org/10.1016/j.matpr.2021.02.132

Smith, M. K., Selbak, H., Wamser, C. C., Day, N. U., Krieske, M., Sailor, D. J., & Rosenstiel, T. N. (2014). Water Cooling Method to Improve the Performance of Field-Mounted, Insulated, and Concentrating Photovoltaic Modules. Journal of Solar Energy Engineering, 136(3). https://doi.org/10.1115/1.4026466

Sudhakar, P., Santosh, R., Asthalakshmi, B., Kumaresan, G., & Velraj, R. (2021). Performance augmentation of solar photovoltaic panel through PCM integrated natural water circulation cooling technique. Renewable Energy, 172, 1433–1448. https://doi.org/10.1016/j.renene.2020.11.138

Tonui, J. K., & Tripanagnostopoulos, Y. (2007). Improved PV/T solar collectors with heat extraction by forced or natural air circulation. Renewable Energy, 32(4), 623–637. https://doi.org/10.1016/j.renene.2006.03.006

Union of Concerned Scientists. (2015). Rooftop Solar Panels: Benefits, Costs, and Smart Policies. https://www.ucsusa.org/clean-

energy/renewable-energy/rooftop-solar-panels-benefits-costs-policies#.WsqAlohuaUk
United Nations. (2016). The World's Cities in 2016: Data Booklet. In Economic and social affair.
Urrego-Ortiz, J., Martínez, J. A., Arias, P. A., & Jaramillo-Duque, Á. (2019). Assessment and Day-Ahead Forecasting of Hourly Solar Radiation in Medellín, Colombia. Energies, 12(22), 4402. https://doi.org/10.3390/en12224402
Verma, S., Mohapatra, S., Chowdhury, S., & Dwivedi, G. (2021). Cooling techniques of the PV module: A review. Materials Today: Proceedings, 38, 253–258. https://doi.org/10.1016/j.matpr.2020.07.130
Vishal Shah, Jerimiah Booream-Phelps, S. M. (2014). 2014 Outlook: Let the Second Gold Rush Begin. Deutsche Bank Markets Reserch. http://www.qualenergia.it/sites/default/files/articolo-doc/DBSolar.pdf
Yusoff, N. F., Zakaria, N. Z., Zainuddin, H., & Shaari, S. (2017). Mounting Configuration Factor for Building Integrated Photovoltaic and Retrofitted Grid-connected Photovoltaic System. Science Letters, 11(1),1–6. https://ir.uitm.edu.my/id/eprint/60284/1/60284.pdf
Zubeer, S. A., & Ali, O. M. (2021). Performance analysis and electrical production of photovoltaic modules using active cooling system and reflectors. Ain Shams Engineering Journal, 12(2), 2009–2016. https://doi.org/10.1016/j.asej.2020.09.022

© 2024. The Author(s). This article is an open access article distributed under the terms and conditions of the Creative Commons Attribution-ShareAlike 4.0 (CC BY-SA) International License (http://creativecommons.org/licenses/by-sa/4.0/)